Experimental Realization of Three-Color Entanglement at Optical Fiber Communication and Atomic Storage Wavelengths

Xiaojun Jia, Zhihui Yan, Zhiyuan Duan, Xiaolong Su, Hai Wang, Changde Xie, and Kunchi Peng[*]

State Key Laboratory of Quantum Optics and Quantum Optics Devices, Institute of Opto-Electronics,
Shanxi University, Taiyuan 030006, People's Republic of China
(Received 30 July 2012; published 18 December 2012)

Entangled states of light including low-loss optical fiber transmission and atomic resonance frequencies are essential resources for future quantum information networks. We present the experimental achievement on the three-color entanglement generation at 852, 1550, and 1440 nm wavelengths for optical continuous variables. The entanglement generation system consists of two cascaded nondegenerated optical parametric oscillators (NOPOs). The flexible selectivity of nonlinear crystals in the two NOPOs and the tunable property of NOPO provide large freedom for the frequency selection of three entangled optical beams. The presented system will hopefully be developed as a practical entangled source to be used in quantum-information networks with atomic storage units and long fiber transmission lines.

Entanglement is the most typical quantum feature that has no analog in classical physics. In modern physics, understanding the conception and property of entanglement continues to attract theoretical and experimental physicists' [1–3] interest, particulary, because it has been demonstrated that quantum entanglement is the most important resource in quantum communication and computation. Many endeavors have prepared various quantum entangled states over the past twenty years [4–11]. A variety of bipartite optical continuous-variable (CV) entangled states have been generated and applied in different protocols of quantum communication involving two parties [6–8]. However, a real quantum information network should be composed of many nodes and channels [9–11]. Controlled quantum communications only can be achieved with the help of multipartite (more than two parties) entangled states. Based on the use of tripartite CV entangled states, interesting quantum communication experiments such as controlled dense-coding [9], quantum teleportation network [10], and quantum secret sharing [11], etc., have been achieved. For practical applications in the real world we have to establish quantum information networks (QINs) involving both light and matter atoms, where light is used for communicating among distant nodes consisting of matter atoms [12]. The atomic systems in network nodes serve as storages of quantum information. The storage and retrieve of quantum states of light are the important operations realizing QINs and have been experimentally demonstrated based on Cs and Rb atoms by several groups [13–17]. For developing practical CV QIN with both storage nodes and fiber transmission lines, it is essential to prepare multipartite entangled states consisting of optical submodes at fiber transmission and atomic transition frequencies.

Nondegenerate optical parametric oscillators (NOPOs) above the threshold are the most successful devices for producing two-color and multicolor CV entangled optical beams in the achieved experiments of quantum optics [18–23]. Two-color entangled optical beams at different frequency regions have been experimentally prepared by means of above-threshold NOPOs with various pump lasers and nonlinear crystals [18–22]. In recent years, for satisfying the requirements of the developing QIN, the generation schemes of multicolor CV entangled states via intra-cavity nonlinear processes have been theoretically proposed [24–27]. In 2009, the first CV three-color entangled state was experimentally produced by an above-threshold NOPO at a low-temperature of −23 °C [23]. The three entangled submodes in this experiment are the output signal and idler and reflected pump modes from a NOPO with wavelengths 1062.102, 1066.915, and 532.251 nm, respectively. It has been theoretically and experimentally demonstrated that the spurious excess phase noise introduced by the nonlinear crystal into the intra-cavity pump field [28,29], which is derived from an influence of phonon noise, will inevitably destroy the phase correlations among the submodes. For reducing the influence of the phonon noise on the reflected pump field, a new scheme of producing three-color entanglement without the use of the reflected pump field is desired. The discrete-variable entangled state of triple photons at three different wavelengths are experimentally produced by a cascaded spontaneous parametric down-conversion process in two different nonlinear crystals [30,31]. Transferring the scheme producing three-color discrete-variable entangled photons to CV regime, our group proposed a generation system of CV three-color entangled optical beams, in which two cascaded NOPO1 and NOPO2 are utilized [26]. The signal beam produced by NOPO1 is used for the pump light of NOPO2, thus the three color entanglement among signal and idler beams produced by NOPO2 and the idler beam output from NOPO1 is theoretically demonstrated and the

optimal operation conditions of the cascaded NOPOs system are numerically calculated in Ref. [26]. Following the theoretical design we have achieved the experimental generation of three-color CV entangled state by using the cascaded NOPOs system for the first time. Through the special selections of the pump laser and the nonlinear crystals in the two NOPOs, the wavelength of one of the obtained three-color entangled beams is 852 nm, which can be tuned to a transition frequency of Cs atoms and thus can be used for the storage of quantum information. The wavelengths of the other two beams are 1550 nm matched for optimal transmission in optical fibers and 1440 nm close to fiber window with quite low (although not optimal) transmission losses [32]. The produced three-color CV entangled states are suitable for applying to future quantum information networks containing both atomic storage unit and optical fiber transmission line.

Figure 1 is the principle schematic of the three-color entanglement generation system, which consists of NOPO1 and NOPO2. The NOPO1 is pumped by a laser (a_0) to create a pair of intense optical beams a_1 and a_2, the frequencies of which fulfill energy conservation $\omega_0 = \omega_1 + \omega_2$, where the subscripts $j = 0, 1, 2$ designate the pump beam and the two generated down-conversion optical beams, respectively. One of the generated optical beams, ($a_p^{in} = a_1^{out}$), drives the NOPO2 to achieve the cascaded intra-cavity optical parametric down-conversion and produces the output fields a_3 (ω_3) and a_4 (ω_4), the frequency sum of which is equal to ω_1 ($\omega_1 = \omega_3 + \omega_4$). It has been theoretically proved in Ref. [26] that the three final output light beams a_2, a_3, and a_4 originating from a single pump beam a_0 have strong intensity correlation. On the other hand, the frequency constraint among the three optical modes translates into a constraint for the phase variations so the phase fluctuations of the optical modes a_1 and a_2 (a_3 and a_4) should be anticorrelated to each other; the sum of their phase fluctuations should be correlated with the phase fluctuation of the pump field. The experimental criteria in terms of the variances of particular combinations of the amplitude and phase quadratures for testing genuine CV multipartite entanglement among optical modes have been given by Loock and Furusawa [33]. A set of the criteria inequalities for determining the CV tripartite entanglement is expressed by
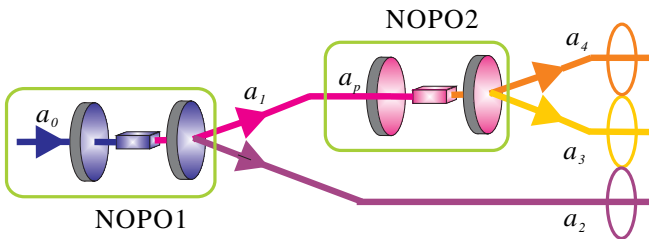
$$\Delta_1 = \langle \delta^2(X_3 - X_4) \rangle + \langle \delta^2(g_1 Y_2 + Y_3 + Y_4) \rangle \geq 4,$$
$$\Delta_2 = \langle \delta^2(X_2 - X_4) \rangle + \langle \delta^2(Y_2 + g_2 Y_3 + Y_4) \rangle \geq 4,$$
$$\Delta_3 = \langle \delta^2(X_2 - X_3) \rangle + \langle \delta^2(Y_2 + Y_3 + g_3 Y_4) \rangle \geq 4, \quad (1)$$

where 4 is the boundary to verify the full inseparability of the genuine tripartite entanglement. The X_j and Y_j ($j = 2$, 3, 4) represent the amplitude quadratures and the phase quadratures of the resultant output modes a_2, a_3, and a_4, respectively. Each pair of X_j and Y_j satisfy the canonical commutation relation $[X_j, Y_j] = 2i$. The g_j ($j = 1, 2, 3$) are the parameter gain factors (arbitrary real parameters), which are chosen to minimize the combined correlation variances at the left side of the inequalities. The theoretical analysis has demonstrated that if any two inequalities in the set of inequalities (1) are simultaneously violated, the three optical modes a_2, a_3, and a_4 are in a CV entangled state [33]. In the experiments we should select the optimal gain factors g_j^{opt} to obtain the minimal correlation variance combinations, which can be accomplished by adjusting the electronic gains of the detected photocurrents as described in Supplemental Material [34].

The experimental setup is shown in Fig. 2. The coherent optical field at 795 nm from a continuous-wave Ti:sapphire laser (MBR110, Coherent Ltd.) is frequency-doubled by a second harmonic generator to obtain the light at 398 nm. Both NOPO1 and NOPO2 are in a Fabre-Perot cavity configuration consisting of two concave mirrors with a 50-mm radius curvature (M1 and M2 for NOPO1, M3 and M4 for NOPO2). For generating the multicolor entangled state satisfying different frequency requirements
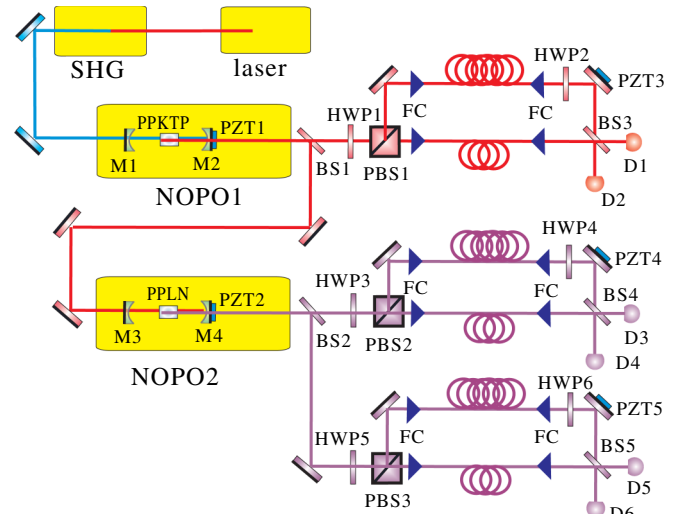

FIG. 2 (color online). Schematic of the experimental setup. Laser: Ti: sapphire laser; NOPO$_{1-2}$: nondegenerate optical parametric oscillator; M$_{1-4}$: different mirror; BS$_{1-5}$: different beam splitter (see context for detailed); HWP: half-wave plate; FC: fiber coupler; PZT$_{1-5}$: piezoelectric transducer; D$_{1-6}$: high-efficiency detector for different wavelength.

FIG. 1 (color online). The principle schematic of the three-color entanglement generation system.

the wavelength difference between the signal and the idler optical beams produced by NOPOs is usually large. The large wavelength difference must result in a large walk-off effect between the two beams and thus significantly decrease the effective interaction length in the nonlinear crystal [35]. The periodically poled crystals have the structure of regularly spaced ferroelectric domains with alternating orientation, which can effectively overcome the harmful walk-off effect [36]. The nonlinear coefficient of periodically poled lithium niobate (PPLN) is higher than that of periodically poled potassium titanyl phosphate (PPKTP), but its absorption loss is larger than that of PPKTP [36,37]. Since the idler output beam of NOPO1 is used for the pump light of NOPO2, its intensity should be higher than the threshold pump power of NOPO2. For producing intense output from NOPO1, the PPKTP with lower absorption loss is chosen for reducing its intra-cavity loss. To NOPO2, we hope that it has the higher parametric conversion efficiency and lower threshold pump power so that the PPLN with the higher nonlinear coefficient is utilized. The size of both PPKTP and PPLN is $1 \times 2 \times 10$ mm^3. The two nonlinear crystals are respectively placed inside an oven, the temperature of which can be independently well controlled and tuned by an electronic temperature controller with the precision of $0.01\,°C$ (YG-IIS-RA, Yuguang Ltd.). M1 (M3) is used for the input coupler of NOPO1 (NOPO2) with the transmissivity of 30% (10%) at 398 nm (746 nm) and the high reflectivity at 746 and 852 nm (1440 and 1550 nm). M2 (M4) is utilized as the output coupler with the high reflectivity at 398 nm (746 nm) and the transmissivity of 3.0% (4.0%) at 746 and 852 nm (1440 and 1550 nm). M2 (M4) is mounted on piezoelectric transducer (PZT1 (PZT2)) for actively scanning the cavity length of NOPO1 (NOPO2), or locking it on the resonance with the generated subharmonic modes as needed. The cavity length, the finesse, and the threshold pump power for NOPO1 (NOPO2) are 101.5 mm (101.9 mm), 195 for 746 nm (149 for 1550 nm), and 75 mW (4.5 mW), respectively.

Three Mach-Zehnder interferometers with unbalanced arm lengths are applied to measure the noise powers of the phase and the amplitude quadratures for the three resultant subharmonic modes at 852 nm (generate by NOPO1), 1440 and 1550 nm (generated by NOPO2), as well as to determine the corresponding quantum noise limits (QNLs) [19,38]. The three interferometers have identical configurations, each of which consists of a polarizing-beam-splitter (PBS1-3), two high reflection mirrors and a 50/50 beam splitter (BS3-5). A PZT (PZT3-5) is mounted on a reflection mirror of the interferometer for locking the relative phase between the long and the short arms of the unbalanced interferometer to the required value. The half wave plate (HWP1-6) is used for aligning the polarization direction of the optical mode. Two polarization-preserved optical fibers with different lengths, in each end-face of

which a fiber coupler is attached, serve as the long and the short arms of the interferometer, respectively. The noise powers of the output optical beams from the interferometers are detected by the photodiodes (D1-D6). For measuring the correlation variance among the three entangled submodes a_2, a_3, and a_4, we first detect the photocurrent noise power of the amplitude quadrature or the phase quadrature of each submode and then combine them with the positive or the negative power combiners according to the requirement of Eq. (1). It has been well proved in Refs. [19,38,39] that when the input optical beams only passes through the short arm of the interferometer, which can be completed by aligning the polarization of the input light to the transmission direction of PBS1-3 with the HWP in front of the PBS, the sum and the difference of the photocurrents detected by a pair of D1 and D2, (also D3 and D4, D5 and D6) are the noise power of the amplitude quadrature of the input beam and the corresponding QNL, respectively. If keeping the optical phase difference between the long and the short arms at $\pi/2 + 2k\pi$ (k is an integer) and splitting equally the input optical beam in the two arms of the interferometer, which can be realized by aligning the polarization of the input light to 45° of PBS1-3 polarization orientation by rotating the HWP, the difference (sum) of the photocurrents detected by a pair of the detectors is the noise power of the phase quadrature of the input beam (corresponding QNL). On the other hand, for implementing the noise power measurement of an input optical beam at a specific noise sideband (f), the phase shift (θ) of the spectral component at $\Omega = 2\pi f$ between the two arms of the Mach-Zehnder interferometer should be controlled at $\theta = n\Omega\Delta L/c = \pi$ (ΔL is the length difference between the two arms; c is the speed of the light; n is the refraction index of the transmission medium) [19,38,39]. For our experiment, the measured noise sideband frequency is $f = 2$ MHz so ΔL should be 48 m. Combining the detected noise powers of the amplitude quadrature X_3 and X_4 (X_2 and X_3; X_2 and X_4) by means of a negative power combiner (not shown in Fig. 2), we obtain the correlation variance $\langle\delta^2(X_3 - X_4)\rangle$ ($\langle\delta^2(X_2 - X_3)\rangle$, $\langle\delta^2(X_2 - X_4)\rangle$). Similarly, adding the noise powers of the phase quadratures with a positive power combiner (not shown in Fig. 3) the correlation variances $\langle\delta^2(g_1^{opt}Y_2 + Y_3 + Y_4)\rangle$ ($\langle\delta^2(Y_2 + g_2^{opt}Y_3 + Y_4)\rangle$; $\langle\delta^2(Y_2 + Y_3 + g_3^{opt}Y_4)\rangle$) is obtained. At last, the combined correlations variances of the amplitude and the phase quadratures are recorded by a spectrum analyzer (not drawn in Fig. 2).

During the experiment, we adjusted the temperature of the PPKTP crystal in the NOPO1 to $23.78\,°C$ first to produce a pair of the signal beam at 746.64 nm and the idler beam at 852.35 nm, which were split by a beam splitter (BS1). The wavelength of the idler beam was at a transition of the Cs atoms exactly. When the pump power at 398 nm was 118 mW, the power of the output subharmonic wave was 17 mW. Tuning the temperature of the
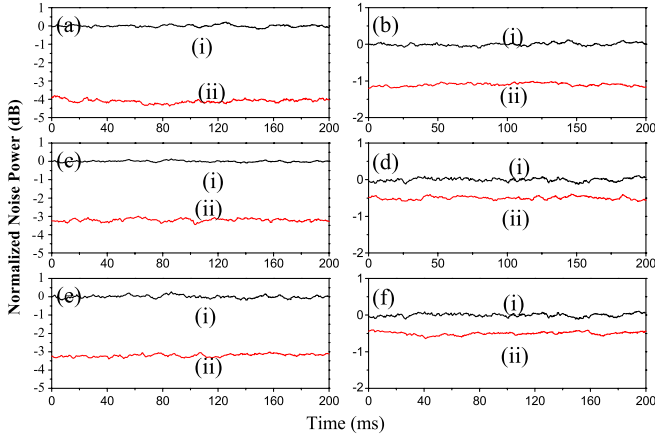
FIG. 3 (color online). The measured correlation variance of three-color entangled states at 2 MHz. a, $\langle\delta^2(X_3 - X_4)\rangle$ b, $\langle\delta^2(g_1^{opt}Y_3 + Y_3 + Y_4)\rangle$, c, $\langle\delta^2(X_2 - X_4)\rangle$, d, $\langle\delta^2(Y_2 + g_2^{opt}Y_3 + Y_4)\rangle$, e, $\langle\delta^2(X_2 - X_3)\rangle$, f, $\langle\delta^2(Y_2 + Y_3 + g_3^{opt}Y_4)\rangle$. (i) The QNL; (ii) The correlation noise power. The resolution and video bandwidths of spectrum analyzer are 30 kHz and 100 Hz, respectively.

PPLN in NOPO2 to 154.0 °C, the wavelength of the signal and the idler beams from the NOPO2 were 1550.60 and 1440.06 nm respectively, which were split by a beam splitter (BS2). Under the pump power of 14.6 mW, the power of the signal (idler) beam from NOPO2 was 3.2 mW.

The measured correlation variances of the noise powers of the amplitude and the phase quadratures among the three resultant optical beams at 852.35, 1550.60, and 1440.06 nm in terms of Eq. (1) are shown in Figs. 3(a)–3(f), where the traces (i) and the traces (ii) stand for the QNLs and the correlation variances, respectively. From Fig. 3 we have $\langle\delta^2(X_3 - X_4)\rangle = -4.1 \pm 0.1 dB$, $\langle\delta^2(g_1^{opt}Y_2 + Y_3 + Y_4)\rangle = -1.1 \pm 0.1 dB$, $\langle\delta^2(X_2 - X_3)\rangle = -3.2 \pm 0.1 dB$, $\langle\delta^2(Y_2 + g_2^{opt}Y_3 + Y_4)\rangle = -0.5 \pm 0.1 dB$, $\langle\delta^2(X_2 - X_4)\rangle = -3.2 \pm 0.1 dB$ and $\langle\delta^2(Y_2 + Y_3 + g_3^{opt}Y_4)\rangle = -0.5 \pm 0.1 dB$, where the minus symbol before the first numbers on the right sides of these equalities means that the variances are below the corresponding QNL and $g_1^{opt} = 0.95 \pm 0.02$, $g_2^{opt} = 1.00 \pm 0.02$, and $g_3^{opt} = 1.00 \pm 0.02$ stand for the optimal gain factors of g_j taken in the experiment for obtaining the highest correlations [33,34]. The three combinations of the correlation variances in Eq. (1) are $\Delta_1 = 3.03 \pm 0.06$, $\Delta_2 = 3.68 \pm 0.05$, and $\Delta_3 = 3.68 \pm 0.05$, respectively, and all of them are smaller than the criterion 4 for the CV three-partite entanglement of optical modes. Thus, the three-color CV entanglement is experimentally demonstrated.

For exhibiting the tunable property of NOPO, we measure the function of the wavelength of the output optical mode from NOPO2 vs the temperature of the nonlinear crystal (Fig. 4). When the temperature of PPLN is changed from 130 °C to 160 °C the measured wavelength of the output signal beam (▲) and idler beam (▼) are changed from 1549.0 and 1441.4 nm to 1550.9 and 1439.8 nm,
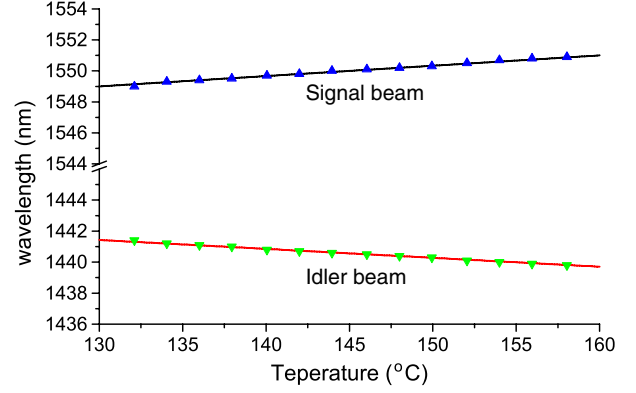

FIG. 4 (color online). Wavelengths of the output signal and idler beams from the NOPO2 changing with the temperature of the PPLN crystal. The solid line is the calculated curve; ▲ and ▼ are the measured wavelengths of the signal and idler beams, respectively.

respectively. The solid lines are theoretically fitting under the idea phase matching condition. The tuned wavelength range is about 1.9 nm for the signal beam. If tuning the temperature of the PPKTP inside NOPO1, the similar tunable property can also be observed. The quality of the three-color entanglement in the total tuning range is almost the same. The agreement between the experimental measurements and the theoretical calculations as well as the perfect linearity of the dependence of the output wavelength on the crystal temperature demonstrate that the NOPO is an idea device for generating the tunable CV entangled states of light.

For the conclusion, we achieve the experimental generation of the three-color CV entangled states of optical modes at the cesium atomic transition and the optical fiber communication frequencies. The results numerically calculated in Ref. [26] show that the physical parameters of the two NOPOs, such as the transmissions of input and output mirrors, the intra-cavity losses, and the pump coefficient σ ($\sigma = \sqrt{P/P_{th}}$, P is the pump power of NOPO, P_{th} is the threshold pump power), simultaneously influence the entanglement quality. For improving entanglement quality the intra-cavity losses of the signal and the idler modes should be reduced. However, the intra-cavity losses of NOPO and the threshold pump power are limited by the quality of the nonlinear crystal and the cavity mirrors. Therefore, for a given experimental system the pump powers of two NOPOs are only adjustable parameters. In the experiments we have to compromisingly choose the pump coefficients of the two NOPOs to obtain the highest entanglement (see Supplemental Material [34] for details). Although the completed entanglement is not very high, the advantage of the wavelengths of the entangled submodes is obvious. For example, if we suppose that −0.2 dB is a cutoff point of entanglements, the achievable maximum transmission distances of entangled states at 1550, 1440,

and 1064 (1080) nm with -3.2 dB amplitude correlation in the optical fiber are 52, 42, and 16 km, respectively (see Supplemental Material [34] for details). According to the CV quantum key distribution scheme in Ref. [40], the obtainable secure bit rate with -3.2 dB amplitude correlation light at 1550 nm is 3 kbits/s against the collective attack after passing through a 20 km optical fiber with the transmission efficiency of 40%. However, if the submode of -3.2 dB correlation at 1064 nm is used, the transmission efficiency in the fiber is only 5% and thus no secure key can be distilled (see Supplemental Material [34] for details).

Using this system, the entangled states can be prepared under normal phase-matching conditions without the need of having to cool the system to below zero degrees [23]. The free selectivity of two nonlinear crystals in the two cascaded NOPOs and the tunable property of NOPO provide large ranges of frequency selection for the three-color entanglement. If NOPOs more than two are cascaded the multicolor CV entangled states with needed frequencies more than three are able to be generated based on the presented method.

---

*kcpeng@sxu.edu.cn

[1] R. Horodecki, P. Horodecki, M. Horodecki, and K. Horodecki, Rev. Mod. Phys. **81**, 865 (2009).

[2] S. L. Braunstein and P. van Loock, Rev. Mod. Phys. **77**, 513 (2005).

[3] M. D. Reid, P. D. Drummond, W. P. Bowen, E. G. Cavalcanti, P. K. Lam, H. A. Bachor, U. L. Andersen, and G. Leuchs, Rev. Mod. Phys. **81**, 1727 (2009).

[4] D. Bouwmeester, J. Pan, K. Mattle, M. Eibl, H. Weinfurter, and A. Zeilinger, Nature (London) **390**, 575 (1997).

[5] Z. Y. Ou, S. F. Pereira, H. J. Kimble, and K. C. Peng, Phys. Rev. Lett. **68**, 3663 (1992).

[6] A. Furusawa, J. L. Sorensen, S. L. Braunstein, C. A. Fuchs, H. J. Kimble, and E. S. Polzik, Science **282**, 706 (1998).

[7] X. Li, Q. Pan, J. Jing, J. Zhang, C. Xie, and K. Peng, Phys. Rev. Lett. **88**, 047904 (2002).

[8] X. Jia, J. Zhang, Y. Wang, Y. Zhao, C. Xie, and K. Peng, Phys. Rev. Lett. **108**, 190501 (2012).

[9] J. Jing, J. Zhang, Y. Yan, F. Zhao, C. Xie, and K. Peng, Phys. Rev. Lett. **90**, 167903 (2003)

[10] H. Yonezawa, T. Aoki, and A. Furusawa, Nature (London) **431**, 430 (2004).

[11] A. M. Lance, T. Symul, W. P. Bowen, B. C. Sanders, and P. K. Lam, Phys. Rev. Lett. **92**, 177903 (2004).

[12] H. J. Kimble, Nature (London) **453**, 1023 (2008).

[13] J. Appel, E. Figueroa, D. Korystov, M. Lobino, and A. I. Lvovsky, Phys. Rev. Lett. **100**, 093602 (2008).

[14] K. Honda, D. Akamatsu, M. Arikawa, Y. Yokoi, K. Akiba, S. Nagatsuka, T. Tanimura, A. Furusawa, and M. Kozuma, Phys. Rev. Lett. **100**, 093601 (2008).

[15] J. Cviklinski, J. Ortalo, J. Laurat, A. Bramati, M. Pinard, and E. Giacobino, Phys. Rev. Lett. **101**, 133601 (2008).

[16] K. Jensen, W. Wasilewski, H. Krauter, T. Fernholz, B. M. Nielsen, M. Owari, M. B. Plenio, A. Serafini, M. M. Wolf, and E. S. Polzik, Nat. Phys. **7**, 13 (2010).

[17] H. Wang, S. Li, Z. Xu, X. Zhao, L. Zhang, J. Li, Y. Wu, C. Xie, K. Peng, and M. Xiao, Phys. Rev. A **83**, 043815 (2011).

[18] A. S. Villar, L. S. Cruz, K. N. Cassemiro, M. Martinelli, and P. Nussenzveig, Phys. Rev. Lett. **95**, 243603 (2005).

[19] X. Su, A. Tan, X. Jia, Q. Pan, C. Xie, and K. Peng, Opt. Lett. **31**, 1133 (2006).

[20] J. Jing, S. Feng, R. Bloomer, and O. Pfister, Phys. Rev. A **74**, 041804 (2006).

[21] G. Keller, V. D'Auria, N. Treps, T. Coudreau, J. Laurat, and C. Fabre, Opt. Express **16**, 9351 (2008).

[22] Y. Li, X. Guo, Z. Bai, and C. Liu, Appl. Phys. Lett. **97**, 031107 (2010).

[23] A. S. Coelho, F. A. S. Barbosa, K. N. Cassemiro, A. S. Villar, M. Martinelli, and P. Nussenzveig, Science **326**, 823 (2009).

[24] A. S. Villar, M. Martinelli, C. Fabre, and P. Nussenzveig, Phys. Rev. Lett. **97**, 140504 (2006).

[25] K. N. Cassemiro and A. S. Villar, Phys. Rev. A **77**, 022311 (2008).

[26] A. Tan, C. Xie, and K. Peng, Phys. Rev. A **85**, 013819 (2012).

[27] Y. Gu, G. He, and X. Wu, Phys. Rev. A **85**, 052328 (2012)

[28] K. N. Cassemiro, A. S. Villar, M. Martinelli, and P. Nussenzveig, Opt. Express **15**, 18 236 (2007).

[29] J. E. S. Cesar, A. S. Coelho, K. N. Cassemiro, A. S. Villar, M. Lassen, P. Nussenzveig, and M. Martinelli, Phys. Rev. A **79**, 063816 (2009)

[30] H. Hubel, D. R. Hamel, A. Fedrizzi, S. Ramelow, K. J. Resch, and T. Jennewein, Nature (London) **466**, 601 (2010).

[31] L. K. Shalm, D. R. Hamel, Z. Yan, C. Simon, K. J. Resch, and T. Jennewein, arXiv:1203.6315.

[32] J. C. Palais, *Fiber Optic Communications* (Prentice Hall, New Jersey, 2004).

[33] P. van Loock and A. Furusawa, Phys. Rev. A **67**, 052315 (2003).

[34] See Supplemental Material at http://link.aps.org/supplemental/10.1103/PhysRevLett.109.253604 for the dependence of the correlation variances on the gain factors, the limitation and the advantage of generated three-color entanglement.

[35] R. W. Boyd, *Nonlinear Optics* (Academic Press, San Diego, 1992).

[36] M. J. Missey, V. Dominic, L. E. Myers, and R. C. Eckardt, Opt. Lett. **23**, 664 (1998).

[37] D. Eger, M. Oron, M. Katz, and A. Zussman, Appl. Phys. Lett. **64**, 3208 (1994).

[38] O. Glockl, U. L. Andersen, S. Lorenz, Ch. Silberhorn, N. Korolkova, and G. Leuchs, Opt. Lett. **29**, 1936 (2004).

[39] D. Wang, Y. Shang, Z. Yan, W. Wang, X. Jia, C. Xie, and K. Peng, Europhys. Lett. **82**, 24 003 (2008).

[40] X. Su, W. Wang, Y. Wang, X. Jia, C. Xie and K. Peng, Europhys. Lett. **87**, 20 005 (2009).